Naval Research Laboratory

Washington, DC 20375-5320

NRL/MR/7140--01-8519

Detection and Classification of Fluctuating Targets

DAVID M. DRUMHELLER

Acoustic Systems Branch
Acoustics Division

HENRY LEW

Defence Science and Technology Organisation
P.O. Box 1500
Salisbury, SA 5108
Australia

March 19, 2001

REPORT DOCUMENTATION PAGE

1. REPORT DATE (DD-MM-YYYY)	2. REPORT TYPE	3. DATES COVERED (FROM - TO)
19-03-2001	Final Report	xx-01-1999 to xx-09-1999

4. TITLE AND SUBTITLE Detection and Classification of Fluctuating Targets Unclassified	5a. CONTRACT NUMBER
	5b. GRANT NUMBER
	5c. PROGRAM ELEMENT NUMBER
6. AUTHOR(S) Drumheller, David M. ; Lew, Henry ;	5d. PROJECT NUMBER
	5e. TASK NUMBER
	5f. WORK UNIT NUMBER
7. PERFORMING ORGANIZATION NAME AND ADDRESS Naval Research Laboratory Washington , DC 20375-5320	8. PERFORMING ORGANIZATION REPORT NUMBER
9. SPONSORING/MONITORING AGENCY NAME AND ADDRESS Office of Naval Research 800 N. Quincy Street Arlington , VA 22217-5660	10. SPONSOR/MONITOR'S ACRONYM(S)
	11. SPONSOR/MONITOR'S REPORT NUMBER(S)

12. DISTRIBUTION/AVAILABILITY STATEMENT
A
PUBLIC RELEASE

Office of Naval Research
800 N. Quincy Street

Arlington , VA 22217-5660

13. SUPPLEMENTARY NOTES

14. ABSTRACT

The structure of echoes observed in echo-location systems such as radar and sonar can exhibit significant variability caused by environmental effects and fluctuations in the target?s aspect. A technique for countering these effects and thereby improving the detection and classification of the target is investigated. The technique relies on being able to characterizes the target?s signal space using a low dimensional signal basis. For this purpose the Karhunen-Loève expansion is used to construct the target?s signal space and in conjunction with the likelihood ratio test form the appropriate test statistic, which is the basis of the detector/classifier structure for distinguishing target returns from nontarget ones. This structure is sometimes referred to as the separable kernel receiver. With this structure in place the performance of the detector/classifier can be evaluated as a function of clutter type and target mismatch. Performance comparisons are also made with a peak detector and a matched filter processor detecting Rayleigh and Rician targets in Rayleigh clutter. The results are presented in the usual form of receiver operating characteristic (ROC) curves.

15. SUBJECT TERMS
classification; detection; signal space

16. SECURITY CLASSIFICATION OF:			**17. LIMITATION OF ABSTRACT**	**18. NUMBER OF PAGES**	**19a. NAME OF RESPONSIBLE PERSON**
			Public Release	24	Fenster, Lynn lfenster@dtic.mil
a. REPORT	**b. ABSTRACT**	**c. THIS PAGE**			**19b. TELEPHONE NUMBER** **International Area Code** **Area Code Telephone Number** 703 767-9007 **DSN** 427-9007
Unclassified	Unclassified	Unclassified			

REPORT DOCUMENTATION PAGE

Form Approved
OMB No. 0704-0188

1. AGENCY USE ONLY (*Leave Blank*)	2. REPORT DATE	3. REPORT TYPE AND DATES COVERED
	March 19, 2001	Final — January 1999 to September 1999

4. TITLE AND SUBTITLE

Detection and Classification of Fluctuating Targets

5. FUNDING NUMBERS

6. AUTHOR(S)

David M. Drumheller and Henry Lew*

7. PERFORMING ORGANIZATION NAME(S) AND ADDRESS(ES)

Naval Research Laboratory
Washington, DC 20375-5320

8. PERFORMING ORGANIZATION REPORT NUMBER

NRL/MR/7140--01-8519

9. SPONSORING/MONITORING AGENCY NAME(S) AND ADDRESS(ES)

Office of Naval Research
800 North Quincy Street
Arlington, VA 22217-5660

10. SPONSORING/MONITORING AGENCY REPORT NUMBER

11. SUPPLEMENTARY NOTES

*Defense Science and Technology Organisation, P.O. Box 1500, Salisbury, SA 5108, Austraila

12a. DISTRIBUTION/AVAILABILITY STATEMENT

Approved for public release; distribution is unlimited.

12b. DISTRIBUTION CODE

13. ABSTRACT (*Maximum 200 words*)

The structure of echoes observed in echo-location systems such as radar and sonar can exhibit significant variability caused by environmental effects and fluctuations in the target's aspect. A technique for countering these effects and thereby improving the detection and classification of the target is investigated. The technique relies on being able to characterizes the target's signal space using a low dimensional signal basis. For this purpose the Karhunen-Loève expansion is used to construct the target's signal space and in conjunction with the likelihood ratio test form the appropriate test statistic, which is the basis of the detector/classifier structure for distinguishing target returns from nontarget ones. This structure is sometimes referred to as the separable kernel receiver. With this structure in place the performance of the detector/classifier can be evaluated as a function of clutter type and target mismatch. Performance comparisons are also made with a peak detector and a matched filter processor detecting Rayleigh and Rician targets in Rayleigh clutter. The results are presented in the usual form of receiver operating characteristic (ROC) curves.

14. SUBJECT TERMS

Classification Signal space
Detection

15. NUMBER OF PAGES

24

16. PRICE CODE

17. SECURITY CLASSIFICATION OF REPORT	18. SECURITY CLASSIFICATION OF THIS PAGE	19. SECURITY CLASSIFICATION OF ABSTRACT	20. LIMITATION OF ABSTRACT
UNCLASSIFIED	UNCLASSIFIED	UNCLASSIFIED	UL

NSN 7540-01-280-5500

Standard Form 298 (Rev. 2-89)
Prescribed by ANSI Std 239-18
298-102

CONTENTS

DETECTION AND CLASSIFICATION OF FLUCTUATING TARGETS

1 INTRODUCTION

The detection and classification of targets using echo-location systems, such as sonar or radar, can be difficult depending on a number of factors. Two of the most important are the environment in which the target operates and the target itself. For example, the environment can produce adverse propagation and clutter[1] to obscure the target, while the target itself can present many different physical, and hence acoustic or electromagnetic, profiles to the echo-location sensor, making its echo potentially difficult to detect and identify on a consistent basis.

Gaumond in a recent paper [1] presented a technique for the detection and classification of a hemispherically end-capped cylindrical shell with periodic internal ribs. The essential idea was to show how deterministic signals from a model of target scattering can be used to develop a detection/classification scheme for a target that has an aspect dependent echo response. In general, the aspect angle of the target was unknown and assumed to be randomly distributed. Therefore it was appropriate to model the target echo as a stochastic signal. This signal was then decomposed into a set of eigenfunctions using the Karhunen-Loève expansion (KLE). It was found that the target echo was well characterised by a small number of KLE terms. These eigenfunctions and their eigenvalues were then used to form a set of filters to detect and classify the target. For this particular case, the stochastic target response was based upon physical components of the echo, e.g., the Bloch and Chalice waves that are readily evident below 1 kHz [2].

The basic idea of this physics-based approach appears to be sufficiently general to allow for adaptation to higher frequencies even though it is no longer obvious what are the relevant physical features that can be used for detection and classification. The purpose of this paper is to extend the KLE technique to high frequencies where physical features may not be readily apparent and the target is embedded in non-Rayleigh clutter. At high frequencies the impulse response of the target echo appears as a superposition of scattering highlights which changes with its aspect. It is hoped that by projecting the target echo response (as a function of aspect angle) onto a signal space representation via the KLE, a useful set of "signal templates" of low dimensionality can result. In effect, the KLE acts as a feature extractor. If this is the case, then it would be of interest to see how the detector/classifier would perform in a highly cluttered environment. A non-Rayleigh representation of the clutter is chosen because of the higher probability of getting large amplitude events mimicking false targets.

Manuscript approved December ??, 2000.

[1] In this report, "clutter" refers to any signal that is composed of a continuous echo from the environment. This term is commonly used in radar parlance. In sonar parlance, the equivalent term is "reverberation."

The outline of the rest of the paper is as follows. In Section 2 the derivation of the test statistic, and therefore the detector/classifier structure, is given. In Section 3 the detector/classifier is applied to a test example. The target, signal and background (clutter) models are specified. This is then followed by a performance evaluation in Section 4 in which receiver operating characteristic (ROC) curves are presented, showing comparisons with the cases of Rayleigh and Rician targets in Rayleigh clutter, as well as a comparison with the peak detector. Furthermore, the detector/classifier's performance as a function of clutter type (from Rayleigh to non-Rayleigh) and target mismatch is also given. Finally, some conclusions and comments are given in Section 5.

2 DETECTOR/CLASSIFIER STRUCTURE

This section reviews the derivation of the detector/classifier structure and explains the motivation and assumptions behind the choice of the structure. The derivation is based on the problem of detecting a coloured Gaussian target in white Gaussian clutter.

A standard and well established way of determining the structure of a detector is to derive the test statistic from the likelihood ratio of the target-plus-clutter and clutter-only probability density functions (PDFs) [3]. Ideally, an optimal detector can be derived if the target and clutter PDFs are known. In practice, this is generally not the case as the characteristics of both the target and clutter can change spatially and temporally for scenarios of operational interest. In some other cases the target and background information may be incomplete or simply not known at all. So instead of seeking an optimal structure it is assumed that, for the purpose of deriving a useful test statistic, the clutter is a zero mean white Gaussian random process and the target is represented by a zero mean coloured Gaussian process. The choice of statistics for the clutter is motivated by the central limit theorem and is thought to represent the limiting case of many situations. Similar considerations follow for the target but with less restrictions on the form of its correlation function (i.e., sample returns from the target response are in general statistically dependent). Clearly, the performance of the detector will be less than optimal once these assumptions are violated, but just like the matched filter, the simplicity of the resultant structure may have the virtues of robustness and utility for a wide range of situations. The usefulness of such a detector can then be tested by subjecting it to a number of non-ideal situations of interest.

By using the above assumptions the detector structure can be derived as follows. To begin, consider the binary detection problem with the null hypothesis (H_0) that no signal is present and the alternative hypothesis (H_1) that the target is present. Symbolically:

$$\begin{aligned} H_0 &: r(t) = n(t) \\ H_1 &: r(t) = s(t) + n(t) \end{aligned} \tag{1}$$

where $r(t)$ is the received waveform, $s(t)$ is a realisation of a zero mean coloured Gaussian process representing the target, and $n(t)$ is a sample waveform of a zero mean white Gaussian process representing the clutter. Note that all waveforms are assumed to be complex valued

for generality. Since the processes are all zero mean Gaussian, their properties can be completely specified by their covariance functions, i.e.,

$$\begin{aligned} E\left\{r(t)r^*(u)|H_0\right\} &= R_n(t,u) \\ E\left\{r(t)r^*(u)|H_1\right\} &= R_s(t,u) + R_n(t,u) \end{aligned} \tag{2}$$

where the signal and clutter are assumed to be independent random processes and

$$\begin{aligned} R_s(t,u) &= E\left\{s(t)s^*(u)\right\} \\ R_n(t,u) &= E\left\{n(t)n^*(u)\right\} = N_0\ \delta(t-u), \end{aligned} \tag{3}$$

with $\delta(\cdot)$ denoting the Dirac delta function. The next step is to expand the signal waveform in terms of an orthonormal series[2]:

$$s(t) = \sum_k s_k \phi_k(t), \tag{4}$$

where

$$s_k = \int \phi_k^*(t) s(t)\ dt \tag{5}$$

and $\{\phi_k(t)\}$ is an orthonormal set of basis functions (specified later), i.e.,

$$\int \phi_k^*(t)\phi_l(t)\ dt = \begin{cases} 1 & \text{for } k = l \\ 0 & \text{for } k \neq l. \end{cases} \tag{6}$$

It therefore follows that the signal waveform is completely specified by its expansion coefficients, s_k, which have the properties:

$$E\left\{s_k\right\} = 0 \tag{7}$$

$$E\left\{s_k s_l^*\right\} = \int\int \phi_k^*(t) R_s(t,u)\phi_l(u)\ dt\, du \tag{8}$$

If the orthonormal basis functions also satisfy

$$\int R_s(t,u)\phi_l(u)\ du = \lambda_l \phi_l(t), \tag{9}$$

then

$$E\left\{s_k s_l^*\right\} = \lambda_l\ \delta_{kl}. \tag{10}$$

Therefore $\{s_k\}$ are a set of independent Gaussian random variables with zero mean and variance, λ_k. The clutter-only waveform can also be expanded using the same set of basis functions so that

$$n(t) = \sum_k n_k \phi_k(t), \tag{11}$$

[2]For simplicity, summations and products written in a form similar to Eq. (4) are indexed from $k = 1$ to ∞. Specific limits will be used when necessary. Similarly, integrals with no limits are definite integrals from $-\infty$ to ∞.

with

$$\begin{aligned} n_k &= \int \phi_k^*(t) n(t)\ dt && (12)\\ E\{n_k\} &= 0 && (13)\\ E\{n_k n_l^*\} &= N_0\ \delta_{kl}. && (14) \end{aligned}$$

Note that the above orthonormal expansion of a random waveform whose basis functions satisfy the integral equation with the covariance function as its kernel is known as the Karhunen-Loève expansion (KLE) [3, 4, 5].

By performing a Karhunen-Loève expansion on the received signal, the binary detection problem becomes

$$\begin{aligned} H_0 &: r_k = n_k \\ H_1 &: r_k = s_k + n_k \end{aligned} \quad (15)$$

where $r(t) = \sum_k r_k \phi_k(t)$ and $r_k = \int \phi_k^*(t) r(t)\ dt$. The PDFs of the null and alternative hypotheses needed to calculate the likelihood function and hence the test statistic are then given by

$$\begin{aligned} f(r(t)|H_0) &= \prod_k \frac{1}{\sqrt{2\pi N_0}} \exp\left\{-\frac{\Re\{r_k\}^2}{2N_0}\right\} \frac{1}{\sqrt{2\pi N_0}} \exp\left\{-\frac{\Im\{r_k\}^2}{2N_0}\right\} \\ &= \prod_k \frac{1}{2\pi N_0} \exp\left\{-\frac{|r_k|^2}{2N_0}\right\} && (16)\\ f(r(t)|H_1) &= \prod_k \frac{1}{2\pi\left(\lambda_k + N_0\right)} \exp\left\{-\frac{|r_k|^2}{2\left(\lambda_k + N_0\right)}\right\}, && (17) \end{aligned}$$

where $\Re\{r_k\}$ and $\Im\{r_k\}$ are the real and imaginary parts respectively. The likelihood function is

$$\begin{aligned} L(r(t)) &\equiv \frac{f(r(t)|H_1)}{f(r(t)|H_0)} \\ &= \left[\prod_l \frac{N_0}{(\lambda_l + N_0)}\right] \exp\left\{\sum_k \frac{\lambda_k}{2N_0(\lambda_k + N_0)} |r_k|^2\right\} && (18) \end{aligned}$$

A detection is declared if the likelihood function is greater than some predetermined decision threshold. It is usual practice to use an equivalent but simpler form of the decision function, the test statistic. For this case, the decision function is simply obtained by taking the logarithm of the likelihood function and keeping only those terms containing the received signal so that the test statistic is

$$T\{r(t)\} = \sum_k \frac{\lambda_k}{(\lambda_k + N_0)} |r_k|^2. \quad (19)$$

Since in some practical situations where the clutter level is unknown, the test statistic can be further simplfied by assuming the worst case of when all the signal components are much smaller than the associated clutter component, i.e., when $\lambda_k \ll N_0$. This results in the test statistic

$$T\{r(t)\} = \sum_k \lambda_k |r_k|^2, \tag{20}$$

which will be adopted as the detector/classifier structure for the remainder of this report. A schematic representation is shown in Fig. 1. It can be seen that this structure has a simple intuitive interpretation, i.e., the detection of the target is determined by a weighted sum of the square of the correlator outputs, where each target basis function acts as a template for the correlation. Note that this structure is also sometimes referred to as the separable kernel receiver [5] because of the properties associated with the kernel of the KLE integral equation (see Eq. (9)).

3 DETECTOR/CLASSIFIER IMPLEMENTATION

3.1 Computing the Basis Functions

The detector/classifier structure derived in the previous section is generic and can be used in many different ways. This section gives a detailed example of applying this structure to an echo location system (e.g., sonar or radar) as a post-processor for discriminating one type of target from the background, i.e., clutter, interference and other targets, etc. A summary of the computational procedure required to implement the post-processor is given as follows:

(1) Generate the covariance matrix of the target response,

$$R_s(i,j) = \frac{1}{N_\theta} \sum_{k=1}^{N_\theta} s(t_i, \theta_k) s^*(t_j, \theta_k), \tag{21}$$

where $s(t_i, \theta_k)$ is the matched filter output of the target echo, θ_k is a random variable representing the aspect angle of the target and N_θ is the number of aspect angles sampled [3].

(2) Solve the eigenvalue problem (the discretized version of the KLE integral equation),

$$\sum_j R_s(i,j)\,\phi_k(j) = \lambda_k \phi_k(i), \tag{22}$$

where $i, j, k = 1, \ldots, L$. In practice, only M of the L most significant eigen-solutions are kept. Of course, this introduces a level of arbitrariness since it has to be decided which eigen-solutions are to be discarded.

[3] This assumes that the PDF of the aspect angles is uniform, which is the most naive assumption that can be made. A more general form of Eq. (21) can be made by removing the factor $1/N_\theta$ and multiplying each term in the summation by the probability of its associated aspect angle.

(3) Use the eigen-solutions, λ_k and $\phi_k(t)$, to compute the test statistic

$$T\{r(t)\} = \sum_{k=1}^{M} \lambda_k \left| \int \phi_k^*(t) r(t)\, dt \right|^2, \tag{23}$$

where $r(t)$ represents the matched filter output of the received waveform for the two cases: target plus background and background only. Sample waveforms from these two cases are used to generate the H_0 and H_1 PDFs of the test statistic. This then allows the decision threshold to be determined by the Neyman-Pearson criterion [3], i.e.,

$$\begin{aligned} T < \gamma \quad &\Rightarrow \quad H_0 \\ T > \gamma \quad &\Rightarrow \quad H_1 \end{aligned} \tag{24}$$

where the decision threshold, γ, is set by the desired false alarm probability.

It is evident from this summary that information about the target, the transmitted signal and background are required for the evaluation of the post-processor's performance. Models of these three areas used to demonstrate the processing are discussed next.

3.2 Target Model

A basic requirement of the above scheme is that the target response as a function of aspect angle be known. This information can be obtained in several ways: field measurements, numerical modelling or measurements using scale models. Each method has its own advantages and disadvantages associated with the computational and measurement difficulties involved. For the purpose of demonstrating the technique, a simple mathematical model of a spatially extended target is used. The model consists of a line of point scatterers, each with a scattering amplitude weighting, w_k, and time delay, τ_k. The important point here is that the target exhibits aspect angle dependence. The far field scattering response of such a target, using a transmitted waveform $x(t)$, is given by

$$y(t) = \int \sum_{k=1}^{N_s} w_k(f) \exp\left[\jmath 2\pi f\,(t - \tau_k)\right] X(f)\, df \tag{25}$$

where

$$\tau_k = \frac{2r}{c_m} + \frac{2(k-1)d}{c_m} \cos\theta, \tag{26}$$

r is the range of the target (assuming a monostatic system), c_m is the speed of wave propagation in the medium, N_s is the number of target highlights, d is the spacing between target highlights, θ is the aspect angle of the target measured relative to the echo-location system's line of sight to the target, $X(f)$ is the Fourier transform of $x(t)$, and $\jmath = \sqrt{-1}$. If the scattering amplitudes of the individual highlights are independent of frequency, then the target response can be simplified to

$$y(t) = \sum_{k=1}^{N_s} w_k\, x(t - \tau_k). \tag{27}$$

It then follows that the matched filter output of the received echo is

$$\begin{aligned} s(t) &= \int y(\xi)x^*(\xi - t)\ d\xi \\ &= \sum_{k=1}^{N_s} w_k \int x(\xi - \tau_k)x^*(\xi - t)\ d\xi. \end{aligned} \tag{28}$$

This then leads to the requirement that the transmitted waveform be specified and hence a discussion of the signal model.

To resolve the target hightlights and thus extract as much information as possible from the target, the use of waveforms with large time-bandwidth products is desirable[4]. A linear frequency modulation (LFM) waveform, which is commonly used in practice, is a particularly simple example of a broadband signal. For mathematical convenience, a LFM waveform with a Gaussian envelope was used in the work reported here. In complex notation, the waveform is given by

$$x(t) = \exp\left(-\frac{t^2}{T_p^2}\right) \exp\left[\jmath 2\pi f_c t + \jmath \frac{\pi B}{T_p} t^2\right], \tag{29}$$

where T_p is the effective pulse length of the signal, f_c is the centre frequency, and B is the bandwidth of the signal. By using Eq. (29) in Eq. (28) the matched filter output of the target echo becomes

$$s(t,\theta) = T_p \sqrt{\frac{\pi}{2}} \sum_{k=1}^{N_s} w_k \exp\left[\jmath 2\pi f_c (t - \tau_k)\right] \exp\left\{-\frac{(1 + (\pi B T_p)^2)}{2T_p^2}(t - \tau_k)^2\right\}. \tag{30}$$

Note that it is usually only the complex envelope of the matched filter that is of interest because of the uncertainties associated with the phase of the carrier signal.

3.3 Clutter Model

In general, the received signal will be contaminated by the background environment so that

$$r(t,\theta) = s(t,\theta) + n(t), \tag{31}$$

where $n(t)$ represents the background field. In the work reported here, It was assumed that the background is dominated by clutter whose behaviour is best modelled as stochastic. In particular, it was assumed that the matched filter output of the clutter has a phase angle that is uniformly distributed and that its amplitude follows the Weibull distribution [6]. The Weibull PDF is given by

$$f_Z(z) = \frac{c z^{c-1}}{b^c} \exp\left[-\left(\frac{z}{b}\right)^c\right], \tag{32}$$

[4]There are many waveforms with large time-bandwidth products have approximately uniform spectra over a frequency interval. Thus, the use of such waveforms means that a target can be interrogated with all frequencies within the system bandwidth. It is in this sense that such waveforms can be used to extract the maximum amount of information from the target. It also justifies the assumption expressed in Eq. (14).

where z is the value of the random variable Z and c and b are the shape and scale parameters respectively. The Weibull distribution is a convenient parametrization of the clutter amplitude as it can represent a wide range of PDFs from Rayleigh ($c = 2$) to non-Rayleigh by the appropriate choice of its shape parameter.

4 PERFORMANCE EVALUATION

The previous section described the computational procedure and the various target, signal and clutter models needed to demonstrate the workings of the separable kernel receiver. Its performance can now be evaluated by choosing the following example set of model parameters.

- The target, composed of a line of point scatterers ($N_s = 15$), is divided into two sets: (i) 10 scatterers, each separated by $d = 0.01$ m, with a scattering amplitude weighting $w_k = 1/50$ and (ii) 5 scatterers, each separated by $d = 10$ m, with $w_k = 1/5$. The propagation speed, c_m, is 1500 m/s.
- The transmitted signal has a carrier frequency, $f_c = 5$ kHz, effective pulse duration, $T_p = 0.01$ s, and bandwidth, $B = 500$ Hz.
- The Weibull clutter parameters are $b = 1/\sqrt{1 + 2/c}$ (normalised power) and c , where c is the free variable.

The target strength (the scattered energy in dB) and the matched filter response are shown in Figs. 2(a) and (b) respectively. The covariance matrix of the target used for the determination of the eigenvalues and eigenvectors of the KLE is constructed from the matched filter response of the target at 5 degree intervals in aspect. The resultant normalised eigenvalues are shown in Fig. 2(c) in descending order of magnitude and the corresponding first five eigenvectors (real part) are shown in Fig. 2(d).

The performance of the separable kernel receiver can be quantified by its ROC curves, specifically, curves of the probability of detection (P_d) as a function of the probability of false alarm (P_{fa}) and signal-to-clutter ratio (SCR), which is generically defined as

$$\text{SCR} = \frac{\text{Peak receiver response to the target echo}}{\text{Expected receiver response to the clutter}} . \tag{33}$$

Therefore, PDFs of the test statistic were estimated by Monte Carlo calculations because analytical methods are generally unavailable except for certain special cases. Specifically, a modified "histogram approach" was used based on importance sampling [7]. One thousand samples were used for each of the target-plus-clutter and clutter-only cases. Furthermore, the target-plus-clutter PDF was obtained by sampling the target response over all aspect angles. For the studies presented in this report, it was assumed that all target aspects are equally likely, but this need not be the case and the problem can be easily modified to suit other situations.

Examples of histograms of the signal-plus-clutter and clutter-only test statistics are shown in Fig. 3 for a SCR equal to 3 dB and 9 dB respectively, and $c = 1.75$ (non-Rayleigh clutter). A realisation of the matched filter output for each case is also shown. These figures show that the separation between the signal-plus-clutter and clutter-only PDFs increase with SCR, as expected. In particular, note that for the case of a SCR equal to 3 dB, the peak values of the clutter response are higher than the peak values of the target response. This demonstrates that if detection is performed by simply comparing the matched filter output to a threshold, there is considerable risk that the target would not be detected and false alarms would occur. Once the PDFs were found, the ROC curves were calculated. An example is shown in Fig. 4 for the target in Weibull clutter with $c = 1.75$ and false alarm probabilities $P_{fa} = 10^{-2}$, 10^{-3} and 10^{-4}. The idealised cases of Rician and Rayleigh fluctuating targets [8] in Rayleigh clutter are also shown in the same figure for comparison. The Rician case corresponds to a non-fluctuating, dominant scatterer in a fluctuating background of a large number of smaller scatterers. The Rayleigh case corresponds to a large combination of scatterers of approximate equal strength. This case also has the useful feature that its ROC curves can be calculated by mostly analytical means. The derivation of the PDFs and their detection and false alarm probabilities are given in the appendix.

The differences between the ROC curves in Fig. 4 can be explained by considering the different assumptions used to derive each detector/classifier. Matched filter receivers only detect energy present in a time series. Knowledge of the target and clutter characteristics is expressed only by the PDFs assumed or derived for the target-plus-clutter and clutter-only cases. For low SCR a non-fluctuating target will almost never rise above the clutter, and for high SCR a fluctuating target will have some significant chance of fading into it. Consequently, for low SCR, the ROC curves for the Rayleigh fluctuating target are higher than those for the non-fluctuating (Rician) target, but for high SCR, they are below them. In deriving the separable kernel receiver, the signal space of the target is used, thus the receiver looks for echoes that have a specific "structure." Consequently, it will tend to ignore large apparent target echoes that do not possess the correct structure, and tend to detect echoes that do even when the SCR is low. Of course, the target echo will fluctuate because the aspect is random. Therefore, it is reasonable that the separable kernel receiver exhibits a higher P_d then either matched filter receiver at low SCR, but does not outperform a matched filter detecting a non-fluctuating target at high SCR.

It is also interesting to compare the performance of the separable kernel receiver with that of a peak detector. The peak detector uses no information about the target and simply searches for the peak of the matched filter output. Figure 5 shows the comparison between the two cases, again indicating that a proper use of target information can significantly improve the detection/classification performance, which in this case is about a 6 dB increase in the SCR when P_d is equal to 0.5.

Next, consider how the separable kernel receiver's performance degrades when there is an adverse clutter distribution. For a fixed P_{fa} equal to 10^{-3}, Fig. 6 shows the ROC curves as a function of the Weibull shape parameter, c, which controls the tail of the clutter PDF ($c = 2$ for Rayleigh, $c = 1$ for Exponential). As in the case for non-Rayleigh behaviour, the longer the tail of the distribution (c decreases), the higher the chance of getting a large amplitude

event that can either mimic target-like features or mask the desired signal. Figure 6 shows the detection performance is severely degraded as the shape of the distribution becomes more exponential in character.

Until now it has been assumed that the target information used to generate the KLE eigenvectors is fairly accurate. In practice, this unlikely to be the case because of a number of factors such as measurement errors, modelling and computational limitations, or distortions of the target response brought about by the operating environment. Figure 7 shows two examples of where the target response (target strength and matched filter output) has been deliberately altered from the original response that was used to construct the KLE eigenvectors. The first case consists of a 10% increase in the scatterer spacing and the removal of one main scatterer. The second case consists of a 50% increase in the scatterer spacing. Figures 8 and 9 show the detection performance of these two cases compared to the matched case. As expected there is a performance degradation, which is manifest as 1.5 to 2 dB effective reduction in SCR for $P_d = 0.5$. This implies that the mismatched separable kernel receivers will still exhibit a higher P_d than the peak detector. Stated alternately, the mismatched separable kernel receiver will exhibit at least a 4 dB effective increase in SCR over the peak detector when $P_d = 0.5$.

5 DISCUSSION AND CONCLUSION

The previous section (see Fig. 5) showed that the separable kernel receiver significantly outperformed the peak detector, i.e., a greater SCR is required for the peak detector to give the same probability of detection as the separable kernel receiver. The peak detector scheme in this case is simply to search for the maximum value of the envelope of the standard matched filter output. This value is proportional to the energy of the target echo. So it is pertinent to ask what is the basis for this performance enhancement in the separable kernel receiver? To answer this, consider the KLE of the signal and clutter waveforms:

$$\begin{aligned} s(t) &= \sum_{k=1}^{\infty} s_k \phi_k(t) \\ n(t) &= \sum_{k=1}^{\infty} n_k \phi_k(t). \end{aligned} \tag{34}$$

The energy of the signal waveform is

$$E_s = \int |s(t)|^2 \; dt = \sum_{k=1}^{\infty} |s_k|^2 \tag{35}$$

and similarly for the clutter waveform, $E_n = \sum_{k=1}^{\infty} |n_k|^2$, where the orthonormal property of the KLE basis functions has been used. The SCR of the peak detector is then given by

$$\mathrm{SCR}_0 \equiv \frac{E_s}{E_n} = \frac{\sum_{k=1}^{\infty} |s_k|^2}{\sum_{k=1}^{\infty} |n_k|^2}. \tag{36}$$

If the signal can be sufficiently characterised by the first N terms of the KLE, i.e.,

$$s(t) \simeq \sum_{k=1}^{N} s_k \phi_k(t), \tag{37}$$

then the energies for the truncated versions of the signal and clutter waveforms are

$$E_s(N) = \sum_{k=1}^{N} |s_k|^2 \simeq E_s \quad \text{and} \tag{38}$$

$$E_n(N) = \sum_{k=1}^{N} |n_k|^2 . \tag{39}$$

Therefore

$$\frac{\mathrm{SCR}(N)}{\mathrm{SCR}_0} \simeq \frac{E_n}{E_n(N)} = \frac{\sum_{k=1}^{\infty} |n_k|^2}{\sum_{k=1}^{N} |n_k|^2} > 1, \tag{40}$$

so that there is an enhancement in the SCR of the truncated signal due to the concentration of the signal energy in a subset of eigenvectors relative to the clutter.

Now consider the case of the separable kernel receiver where its outputs for the signal and clutter components are

$$T\{s(t)\} = \sum_{k=1}^{M} \lambda_k |s_k|^2 \quad \text{and} \tag{41}$$

$$T\{n(t)\} = \sum_{k=1}^{M} \lambda_k |n_k|^2 . \tag{42}$$

Then define the SCR of the separable kernel receiver output as

$$\mathrm{SCR}_T \equiv \frac{T\{s(t)\}}{T\{n(t)\}} \tag{43}$$

so that

$$\frac{\mathrm{SCR}_T}{\mathrm{SCR}_0} = \frac{\sum_{k=1}^{M} \lambda_k |s_k|^2}{\sum_{k=1}^{\infty} |s_k|^2} \cdot \frac{\sum_{k=1}^{\infty} |n_k|^2}{\sum_{k=1}^{M} \lambda_k |n_k|^2}. \tag{44}$$

Let the eigenvalues, λ_k, be normalised to their largest value and placed in descending order. If the signal energy is essentially confined to a finite number of eigenvectors, as indicated by the decay of the eigenvalues, then

$$\sum_{k=1}^{M} \lambda_k |s_k|^2 \simeq \sum_{k=1}^{\infty} |s_k|^2 \tag{45}$$

and by the same argument as above,

$$\frac{\mathrm{SCR}_T}{\mathrm{SCR}_0} > 1. \tag{46}$$

In effect, the eigenvalues provides a softer, less abrupt truncation of the signal expansion than would otherwise be the case for a simple termination of the series. However, the enhancement in the SCR in both cases comes from the compact nature of the signal energy when the signal is decomposed according to the KLE basis functions.

In conclusion, this report presents a technique for the detection and classification of complex targets whose echoes are strongly sensitive to the target's aspect dependence. It has been shown that a priori information about the target can be used to enhance the detection and classification performance. The KLE was used to form the basis of a receiver structure that exploited the compactness of the signal's energy relative to that of the background. In addition, the KLE has the advantage of providing a "natural" signal space basis into which the received waveform can be decomposed. This signal decomposition was achieved by solving the eigenvalue problem associated with the KLE of the target signal. The resultant eigenvectors, weighted by their eigenvalues, played the role of templates for the detection and classification of the target.

6 ACKNOWLEDGMENTS

The authors are grateful to Dr. Charles F. Gaumond of the Naval Research Laboratory, Washington, DC for informative discussions on the Karhunen-Love expansion and the separable kernel receiver. They are also grateful to Dr. Richard M. Ellem of the Defence Science and Technology Organisation, Salisbury, South Australia for assisting with the typesetting of this report.

This work was sponsored by the Office of Naval Research.

The authors may be contacted at the following e-mail addresses: *henry.lew@dsto.defence.gov.au* and *drumheller@nrl.navy.mil*.

7 REFERENCES

[1] C. F. Gaumond, "Echo Components for Aspect-Independent Detection and Classification," *IEEE J. Oceanic Eng.*, **24**, No. 4, pp. 436-446, October 1999.

[2] L. R. Dragonette, et al, "The application of two-dimensional signal transformations to the analysis and synthesis of structural excitations observed in acoustical scattering," *Proceedings of the IEEE*, **84**, No. 9, pp. 1249-1263, September 1996.

[3] A. D. Whalen, *Detection of Signals in Noise*, Academic Press, New York, 1971.

[4] C. W. Helstrom, *Statistical Theory of Signal Detection*, Pergamon Press, Oxford, 1968.

[5] H. L. Van Trees, *Detection, Estimation and Modulation Theory, Vol. 1*, Wiley, New York, 1971.

[6] M. Sekine and Y. Mao, *Weibull Radar Clutter*, Peter Peregrinus, London, 1970.

[7] R. L. Mitchell, "Importance Sampling Applied to Simulation of False Alarm Statistics," *IEEE Trans. Aerospace and Electronic Systems,* **AES-17**, No. 1, pp. 15-24, January 1981.

[8] M. I. Skolnik, *Introduction to Radar Systems*, McGraw-Hill, New York, 1962.

APPENDIX

PROBABILITY DENSITY FUNCTION OF THE SEPARABLE KERNEL RECEIVER OUTPUT

This appendix outlines the derivation of the probability density functions (PDFs) and their corresponding detection and false alarm probabilities of the separable kernel receiver for the case of a fluctuating Rayleigh target in Rayleigh clutter. Recall that the test statistic for the separable kernel receiver is

$$T\{r(t)\} = \sum_{k=1}^{M} \lambda_k \left|r_k\right|^2 \tag{A1}$$

and so the aim is to obtain the PDFs of T for both the target-plus-clutter and clutter only cases. To begin, assume that the in-phase ($\Re\{r_k\}$) and the quadrature ($\Im\{r_k\}$) components of the received waveform follow a zero mean Gaussian distribution with the variance given by

$$\begin{array}{lcll} H_0 & : & \sigma_k^2 = N_0 & \text{(clutter only)} \\ H_1 & : & \sigma_k^2 = \lambda_k + N_0 & \text{(target plus clutter).} \end{array} \tag{A2}$$

Then the PDF of the amplitude of r_k is

$$f\left(|r_k|\right) = \frac{|r_k|}{\sigma_k^2} \exp\left\{-\frac{|r_k|^2}{2\sigma_k^2}\right\}. \tag{A3}$$

It is convenient to introduce a change of variables so that the test statistic is $T = \sum_{k=1}^{M} u_k$, where $u_k = \lambda_k \left|r_k\right|^2$. The PDF of the new random variable then becomes

$$g\left(u_k\right) = \frac{1}{2\lambda_k\sigma_k^2} \exp\left\{-\frac{u_k}{2\lambda_k\sigma_k^2}\right\} \tag{A4}$$

and its corresponding characteristic function for u_k is

$$\begin{aligned} \Phi_{u_k}(t) &= \int_{-\infty}^{\infty} g(u_k) e^{\jmath u_k t}\, du_k \\ &= \frac{1}{1 - \jmath 2\lambda_k\sigma_k^2 t}, \end{aligned} \tag{A5}$$

where $\jmath = \sqrt{-1}$. Therefore, the characteristic function for T is

$$\begin{aligned} \Phi_T(t) &= \prod_{k=1}^{M} \Phi_{u_k}(t) \\ &= \sum_{k=1}^{M} \frac{A_k}{1 - j2\lambda_k \sigma_k^2 t}, \end{aligned} \tag{A6}$$

where A_k are the residues of the partial fraction expansion of the product (assuming no degeneracy in the poles). By taking the inverse Fourier transform of the characteristic function, the PDF of the test statistic is

$$f_T(T) = \sum_{k=1}^{M} \frac{A_k}{2\lambda_k \sigma_k^2} \exp\left\{ -\frac{T}{2\lambda_k \sigma_k^2} \right\} \tag{A7}$$

and the false alarm and detection probabilities are given by

$$\begin{aligned} P_T(T) &= \int_T^{\infty} f_T(t)\, dt \\ &= \sum_{k=1}^{M} A_k \exp\left\{ -\frac{T}{2\lambda_k \sigma_k^2} \right\} \end{aligned} \tag{A8}$$

for each of the two cases given in Eq. (A2). This last set of equations allows the detection threshold to be determined for a given false alarm probability. This may be accomplished using Newton's method. The threshold can also be used to calculate the probability of detection.

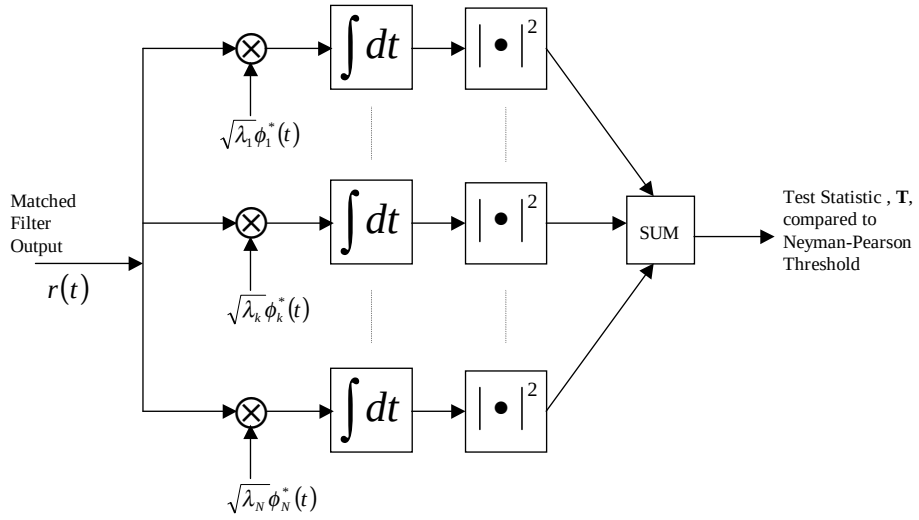

Figure 1: The structure of the separable kernel receiver.

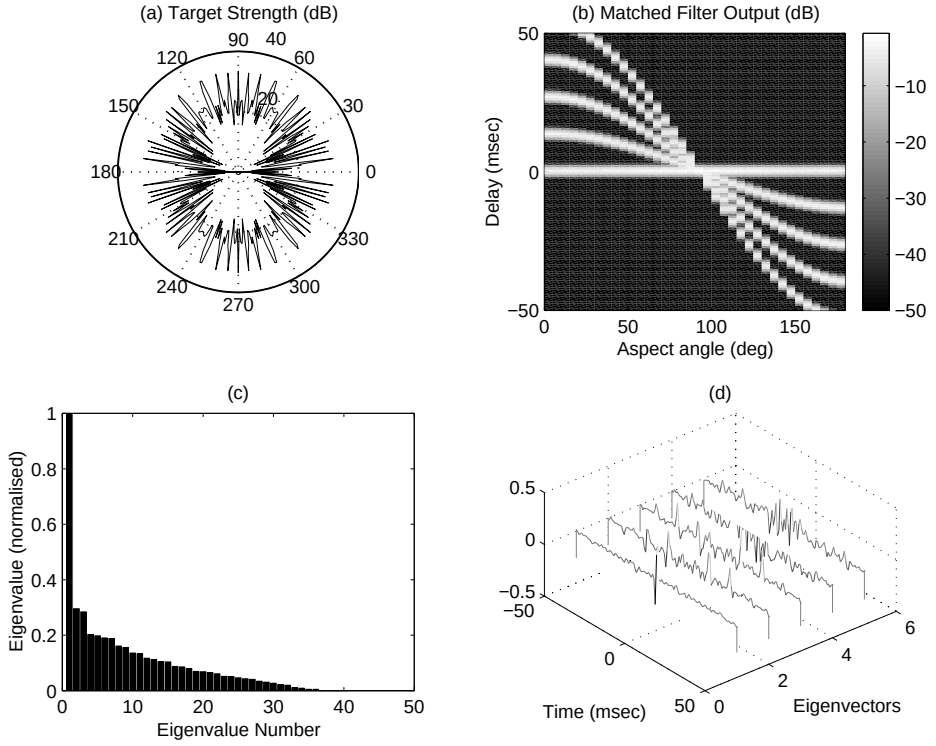

Figure 2: Some properties of the target response: (a) target strength as a function of aspect, (b) matched filter output as a function of aspect, (c) the eigenvalues of the KLE, and (d) the corresponding first five eigenvectors of the KLE.

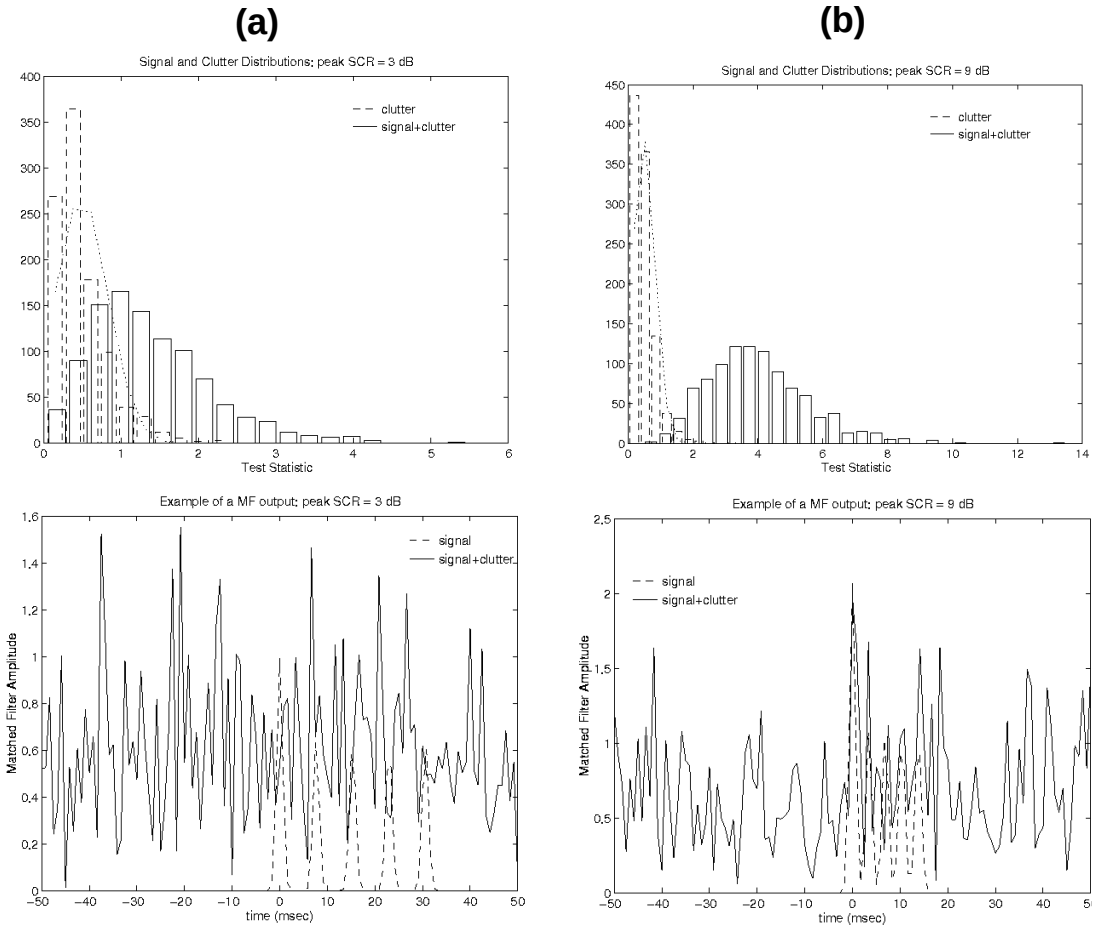

Figure 3: The histograms of the signal-plus-clutter and clutter-only test statistics for two cases of SCR: (a) 3 dB and (b) 9 dB. An example of a matched filter output realization is also shown for each case.

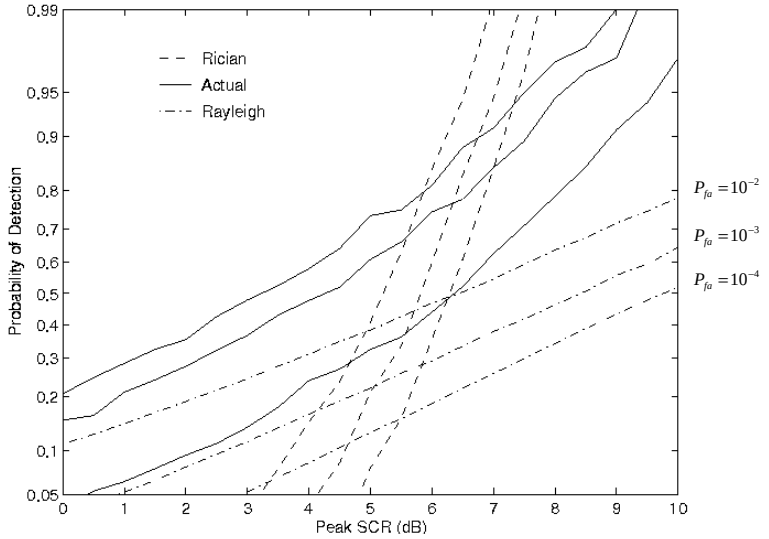

Figure 4: Three sets of ROC curves show the performance of the separable kernel receiver for: (solid lines) the target in Weibull clutter ($c = 1.75$), (broken lines) a Rician fluctuating target in Rayleigh clutter, and (dash-dot lines) a Rayleigh fluctuating target in Rayleigh clutter. Within each set, each curve corresponds to a false alarm probability of 10^{-2}, 10^{-3} and 10^{-4} from left to right.

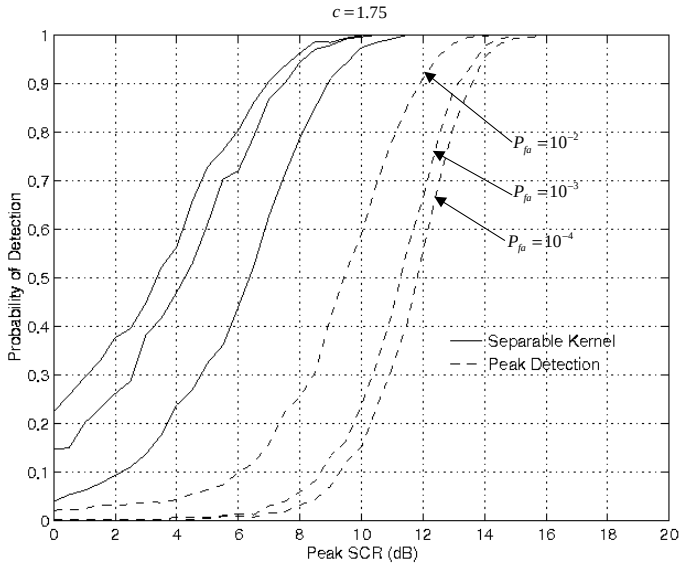

Figure 5: The ROC curves of the separable kernel receiver (solid lines) and the peak detector (broken lines) for falsm alarm probabilities of 10^{-2}, 10^{-3} and 10^{-4} in Weibull clutter ($c = 1.75$).

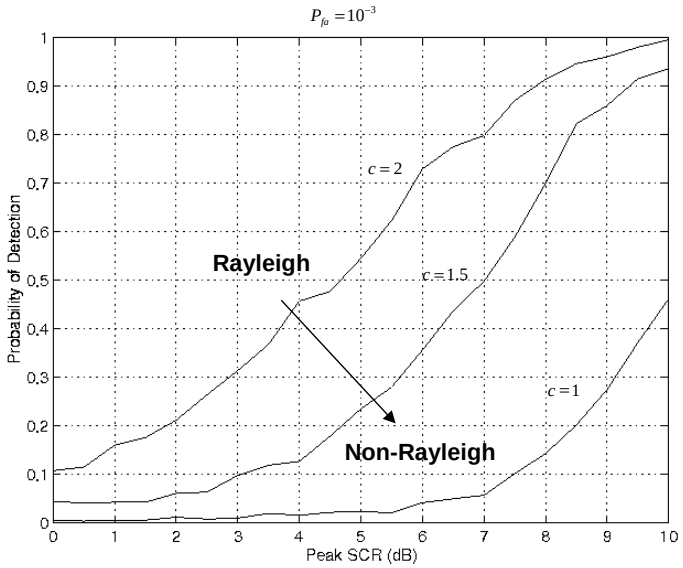

Figure 6: The ROC curve of the separable kernel receiver as a function of the Weibull shape parameter for a false alarm probability of 10^{-3}.

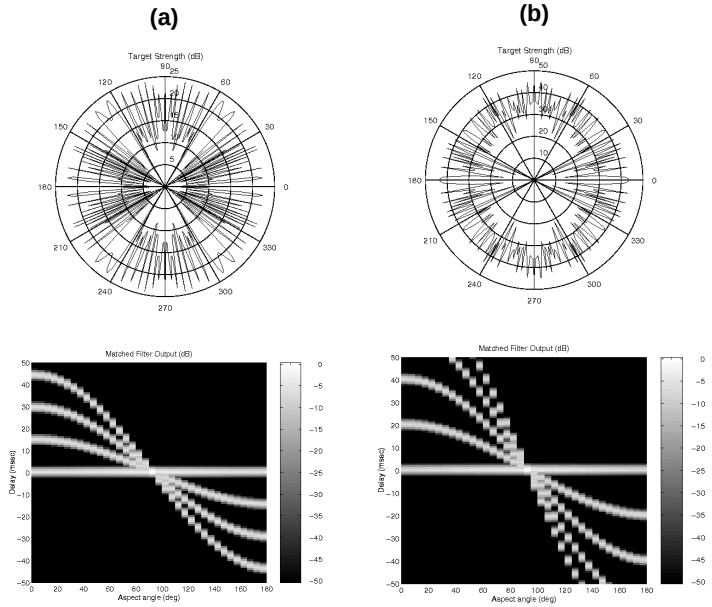

Figure 7: The target strength and matched filter output as a function of aspect for two cases: (a) the spacing between the main scatterers is increased by 10% with one less scatterer; and (b) the spacing between scatterers is increased by 50%.

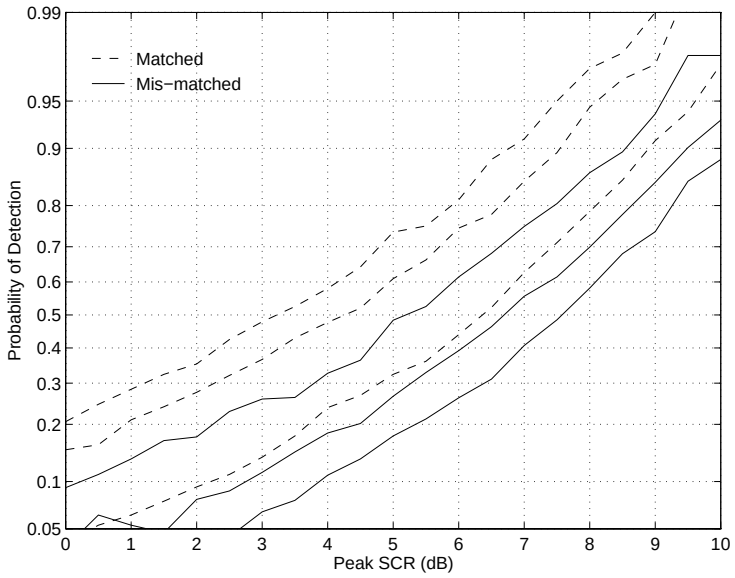

Figure 8: The ROC curves of the separable kernel receiver showing the degradation in performance when there is a 10% mismatch in the scatterer spacing and one less main scatterer.

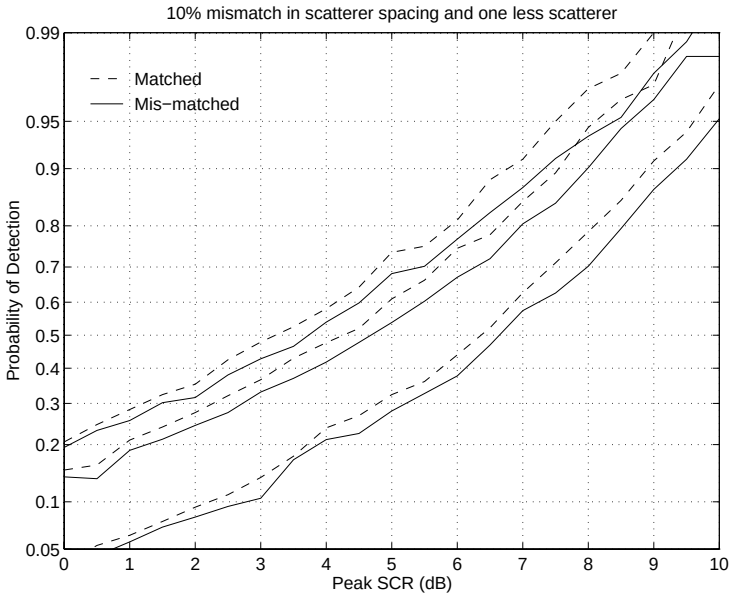

Figure 9: The ROC curves of the separable kernel receiver showing the degradation in performance when there is a 50% mismatch in the scatterer spacing.